1   **Low base-substitution mutation rate in the germline genome of the**

2   **ciliate *Tetrahymena thermophila***

3   Hongan Long[1,2,a], David J. Winter[3,a,*], Allan Y.-C. Chang[1], Way Sung[4], Steven H. Wu[3], Mariel Balboa[1],

4   Ricardo B. R. Azevedo[1], Reed A. Cartwright[3,5], Michael Lynch[2], Rebecca A. Zufall[1]

5   1. Department of Biology and Biochemistry, University of Houston, Houston, Texas 77204-5001, USA.

6   2. Department of Biology, Indiana University, Bloomington, Indiana 47405-7005, USA.

7   3. The Biodesign Institute, Arizona State University, Tempe, Arizona 85287-5301, USA.

8   4. Department of Bioinformatics and Genomics, University of North Carolina at Charlotte, Charlotte,
9   North Carolina 28223-0001, USA.

10   5. School of Life Sciences, Arizona State University, Tempe, Arizona 85287-5301, USA.

11   a. These authors contributed equally to this work.

12   * To whom correspondence may be addressed. Email: djwinter@asu.edu

13

14

ABSTRACT

Mutation is the ultimate source of all genetic variation and is, therefore, central to evolutionary change. Previous work on *Paramecium tetraurelia* found an unusually low germline base-substitution mutation rate in this ciliate. Here, we tested the generality of this result among ciliates using *Tetrahymena thermophila*. We sequenced the genomes of 10 lines of *T. thermophila* that had each undergone approximately 1,000 generations of mutation accumulation (MA). We applied an existing mutation-calling pipeline and developed a new probabilistic mutation detection approach that directly models the design of an MA experiment and accommodates the noise introduced by mismapped reads. Our probabilistic mutation-calling method provides a straightforward way of estimating the number of sites at which a mutation could have been called if one was present, providing the denominator for our mutation rate calculations. From these methods, we find that *T. thermophila* has a germline base-substitution mutation rate of 7.61×10^{-12} per-site, per cell division, which is consistent with the low base-substitution mutation rate in *P. tetraurelia*. Over the course of the evolution experiment, genomic exclusion lines derived from the MA lines experienced a fitness decline that cannot be accounted for by germline base-substitution mutations alone, suggesting that other genetic or epigenetic factors must be involved. Because selection can only operate to reduce mutation rates based upon the "visible" mutational load, asexual reproduction with a transcriptionally silent germline may allow ciliates to evolve extremely low germline mutation rates.

Key words: mutation accumulation, micronucleus, macronucleus, drift-barrier hypothesis, microbial eukaryote, Oligohymenophorea.

INTRODUCTION

36

37   Mutation is the ultimate source of all genetic variation, and the rate, molecular spectrum, and phenotypic

38   consequences of new mutations are all important drivers of biological processes such as adaptation, the

39   evolution of sex, the maintenance of genetic variation, aging, and cancer. However, because mutations are

40   rare, detecting them is difficult, often requiring the comparison of genotypes that have diverged from a

41   common ancestor by at least hundreds or thousands of generations. Further, interpreting the results of

42   such comparisons is complicated by the fact that mutations are frequently eliminated by natural selection

43   before they can be studied.

44   Mutation accumulation (MA) is a standard method for studying mutations experimentally. In a

45   typical MA experiment, many inbred or clonal lines are isolated and passed repeatedly through

46   bottlenecks. This reduces the effective population size and lessens the efficiency of selection, allowing all

47   but the most deleterious mutations to drift to fixation (Bateman 1959; Mukai 1964). The genome-wide

48   mutation rate and mutational spectrum can then be estimated by comparing the genomes of MA lines with

49   those of their ancestors. Such direct estimates of mutational parameters are now available for a number of

50   model organisms (Denver et al. 2009; Keightley 2009; Keightley et al. 2014; Lee et al. 2012; Lind and

51   Andersson 2008; Lynch et al. 2008; Ness et al. 2012; Ossowski et al. 2010; Sung et al. 2012b; Zhu et al.

52   2014). However, the narrow phylogenetic sampling of these species still limits our ability to understand

53   how mutation rates and patterns have evolved and, in turn, have influenced evolution across the tree of

54   life.

55   Microbial eukaryotes are an extraordinarily diverse group, containing many evolutionarily distant

56   lineages, some of which have unusual life histories and genome features (Katz and Bhattacharya 2006).

57   However, microbial eukaryotes are often unsuitable for use in mutational studies because they are

58   difficult to culture in the lab, especially at the small population sizes required to reduce the efficiency of

59   selection in MA experiments. In addition, genomic resources (e.g., completed annotated reference

3

60 genomes) are lacking for most eukaryotic microbes. These barriers have limited MA experiments to well-

61 annotated model microbial eukaryotes such as *Saccharomyces cerevisiae* (Lynch et al. 2008; Zhu et al.

62 2014), *Schizosaccharomyces pombe* (Behringer and Hall 2015; Farlow et al. 2015), *Paramecium*

63 *tetraurelia* (Sung et al. 2012b)*, Dictyostelium discoideum* (Saxer et al. 2012)*,* and *Chlamydomonas*

64 *reinhardtii* (Ness et al. 2012; Ness et al. 2015; Sung et al. 2012a; fig. 1).

65 The ciliated unicellular eukaryote *Tetrahymena thermophila* is well suited to MA experiments.

66 Like all ciliates, individuals from this species have distinct germline and somatic copies of their nuclear

67 genome. During asexual growth, the contents of the germline genome are duplicated mitotically but are

68 neither expressed nor used to generate a new somatic genome. But unlike most other ciliates (including *P.*

69 *tetraurelia*, which senesces in the absence of periodic mating or autogamy), *T. thermophila* can be

70 propagated this way indefinitely. Thus, during periods of asexual growth — which can last over

71 thousands of generations (Doerder 2014) — mutations can accumulate in the germline genome without

72 being exposed to natural selection, which is operating on the somatic genome. Long et al. (2013)

73 confirmed that MA lines of *T. thermophila* can be propagated asexually for at least 1,000 generations and

74 inferred that they accumulate mutations in their germline genomes with detectable effects on fitness after

75 the mutations are expressed in the somatic genome. However, Long et al. (2013) did not estimate the

76 mutation rate directly at the molecular level.

77 The only other existing MA experiment from a ciliate was performed on *Paramecium tetraurelia*

78 (Sung et al. 2012b) and yielded the lowest known base-substitution mutation rate in a eukaryote. Sung et

79 al. (2012b) suggested that this exceptionally low mutation rate is the result of the unusual life history of

80 ciliates, in which a transcriptionally silent germline genome undergoes multiple rounds of cell division

81 between sexual cycles. Measurement of the mutation rate of *T. thermophila* will help reveal whether a

82 low mutation rate is a general feature of ciliates. In addition, natural populations of *T. thermophila* have

83 been the focus of population-genetic studies (Katz et al. 2006; Zufall et al. 2013), so mutational

84 parameters estimated from MA experiments can be related to population and evolutionary processes.

4

85   Although the life history of *T. thermophila* is ideal for MA experiments, some features of its

86   genome complicate typical computational approaches to detecting mutations from short-read sequencing.

87   The genome is extremely AT-rich (~78% AT), contains many low complexity and repetitive elements,

88   and has an incomplete reference genome (Eisen et al. 2006). These features make mapping sequencing

89   reads to the reference genome difficult, which may lead to false positives when using naive mutation

90   detection methods. To overcome these difficulties, we have developed a novel probabilistic mutation

91   detection approach that directly models the design of an MA experiment and accommodates the noise

92   introduced by mismapped reads. We used both our new method and an existing mutation-calling pipeline

93   (Sung et al. 2012b) to analyse the MA sequences.

94   Here we expand the work presented by Long et al. (2013) by directly estimating the base-

95   substitution mutation rate in *T. thermophila*. Our results are consistent with the exceptionally low rate

96   estimated for *P. tetraurelia*, indicating that low germline mutation rates may be a general feature of

97   ciliates. We also use our estimated rate to calculate the effective population size of *T. thermophila* in the

98   wild. Our results establish that it is possible to estimate the mutation rate of *T. thermophila* directly from

99   sequence data, but owing to the extraordinarily low rate, longer and larger MA experiments will be

100   required to confidently estimate the mutational spectrum of a species with such a low mutation rate.

101

MATERIALS AND METHODS

Cell lines

104   The 10 evolved cell lines that were used in this study were generated from 10 parental MA lines

105   (Supplementary Table S1). These lines were established from a single cell of the strain SB210 as

106   described in Long et al. (2013). Briefly, the 10 MA lines were cultured in rich medium (SSP) in test tubes

107   (Gorovsky et al. 1975) and experienced ~50 single-cell bottlenecks and ~1000 cell divisions, except for

108   M28, which was bottlenecked 10 times and passed ~200 cell divisions. The optical density of cultures

109   was measured prior to each transfer and the number of generations calculated using a standard curve of

110   optical density for the ancestor (Long et al. 2013). Because directly sequencing the *T. thermophila*

111   micronuclear genome is not feasible, we generated autozygous lines with macronuclear genomes derived

112   from haploid copies of our ancestral and descendant micronuclear genomes using genomic exclusion

113   (Allen 1963). Genomic exclusion lines were produced by two rounds of crossing between the MA lines

114   (mating type VI) and a germline-dysfunctional B* strain (mating type VII, Bruns and Cassidy-Hanley,

115   1999). A mutation in the macronuclear genome of a genomic exclusion line derived from an MA line is

116   assumed to correspond to a germline mutation in that MA line.

117   We accounted for heterozygosity in the ancestral strain by generating 19 independent genomic

118   exclusion lines from the progenitor line. The DNA from all 19 genomic exclusion lines was pooled before

119   library construction, allowing us to sequence both alleles at any heterozygous sites.

Whole-genome sequencing

121   DNA libraries with insert size ~350 bp were constructed and Illumina paired-end sequenced by the

122   DNASU core facility at the Biodesign Institute at Arizona State University and the Hubbard Center for

123   Genome Studies, University of New Hampshire. The mean sequencing depth is ~47×, with >90% of the

124   sites in the genome covered in all the sequenced lines (Supplementary Table S1). Sequencing reads are

125   available from the NCBI's SRA database under a BioProject with accession number PRJNA285268.

Base-substitution analysis

127   We used two independent approaches to call point-mutations to avoid false negatives that might not be

128   detected by a single approach. First, a widely used consensus approach (Sung et al. 2012b). Second, a

129   probabilistic approach that adapts methods designed for family-based data to the design of MA

130   experiments (Cartwright et al. 2012). Our list of candidates was generated by the union of calls from both

131   methods.

132 *Consensus approach*

133 For the consensus approach we applied the following filters to reduce false positives that may arise from

134 sequencing, read mismapping or library amplification errors. (1) Two mapping programs, BWA 0.7.10

135 (Li and Durbin 2009) and novoalign (V2.08.01; NOVOCRAFT Inc), were used in two independent

136 pipelines to reduce algorithm-specific read mapping errors. (2) Only uniquely mapped reads were used

137 (BWA option: sampe –n 1; NOVOCRAFT option: novoalign –r None), with mapping/sequencing quality

138 scores > 20 (samtools mpileup –Q 20 –q 20). (3) The line-specific consensus nucleotide at a genomic site

139 needed support from greater than 80% of reads to filter out false positives from mismapping of paralog

140 reads. (4) Three forward and three reverse reads were required to determine the line-specific consensus

141 nucleotide, to reduce false positive calls due to errors in library construction or sequencing. Putative

142 mutations were then called if a single line was different from the consensus of all the remaining lines

143 following the approach of Sung et al. (2012b). This approach has been applied to a wide variety of

144 prokaryotic and eukaryotic organisms and repeatedly verified with Sanger sequencing (Denver et al.

145 2009; Lee et al. 2012; Long et al. 2015; Ossowski et al. 2010; Sung et al. 2015). The consensus approach

146 also makes predictions consistent with those of the GATK SNP caller (Behringer and Hall 2015; Farlow

147 et al. 2015).

148 *Probabilistic approach using accuMUlate*

149 The challenge of identifying mutations from genomic alignments can also be treated as a hidden-data

150 problem (Cartwright et al. 2012). Fig. 2 illustrates the application of a hidden-data approach to our MA

151 experiment. For a given site in the reference genome, the only data we observe directly is the set of

152 sequencing reads mapped to that site. In order to determine if a mutation has occurred at the site, we have

153 to consider the processes by which the read data was generated. These processes include biological

154 processes (e.g., inheritance, mutation, genomic exclusion) and experimental processes that can introduce

155 errors (e.g., library preparation, sequencing, data processing). Because none of these states are directly

156 observed, we consider them to be hidden data. Each unique combination of hidden states represents a

7

157   distinct history that could have generated the read data for a given state. See fig. 3 for an example of one

158   such history with hidden and observed data illustrated.

159   With the above formulation, our challenge is to determine the probability that a site contains at

160   least one *de novo* mutation using our sequencing data (R) as the only observed input

161   *(1)*

162
$$P(\text{mutation}|R;\Theta) \ = \ \frac{P(\text{mutation}, R;\Theta)}{P(R;\Theta)}.$$

163   Here, $P(\text{mutation}, R;\Theta)$ is the joint marginal probability of at least one mutation being present and the

164   sequencing data, and $P(R;\Theta)$ is the marginal probability of the sequencing data. The parameter Θ

165   represents the model parameters and consists of the following:

166   • θ, the proportion of sites in the ancestor that are heterozygous, approximately (see Equation 6);
167   • φ_A, the overdispersion parameter for sequencing of the ancestor (described below);
168   • φ_D, the overdispersion parameter for sequencing of the descendant lines (described below);
169   • $\boldsymbol{\pi}$, a vector representing the frequency of each nucleotide in the ancestral genome;
170   • μ, the experiment-long mutation rate per site;
171   • ε, the rate of sequencing error per site.

172   The numerator and denominator in Equation 1 are marginal probabilities. To calculate them from the full

173   data we have to sum the probability of mutation over the full set of histories (H). Each of these histories is

174   a unique combination of hidden states that could have generated the read data (an example of one such

175   history is shown in fig. 3),

176   *(2)*

177
$$P(\text{mutation}|R;\mathit{\Theta}) \ = \ \frac{\sum_{h\in H} P(\text{mutation}, R, h;\Theta)}{\sum_{h\in H} P(R, h;\Theta)}$$

178
$$= \ \frac{\sum_{h\in H} P(\text{mutation} \mid h)\, P(R, h;\mathit{\Theta})}{\sum_{h\in H} P(R, h;\mathit{\Theta})}.$$

179   Note that the probability of there being at least one mutation in a given history h, $P(\text{mutation} \mid h)$, is

180   known to be either 1 or 0. Therefore, we only need to calculate $P(R, h;\Theta)$, the probability of the full data

181   for the set of model parameters. This amounts to finding the probability that the read data was generated

182   from an ancestral genotype G_A that gave rise to descendants with genotypes specified by the particular

183   history being considered. This can be calculated as the products of the prior probability of genotypes and

184   the likelihoods of those genotypes given the set of all sequencing data (R),

185   *(3)*

186

$$P(R, h; \Theta) = \underbrace{P(G_A; \theta, \boldsymbol{\pi})}_{a} \cdot \underbrace{P(\boldsymbol{R_A}| G_A; \varphi_A, \varepsilon)}_{b} \cdot \prod_{i}^{n} \left[\underbrace{P(G_i \mid G_A; \boldsymbol{\pi}, \mu)}_{c} \cdot \underbrace{P(\boldsymbol{R_i} \mid G_i; \varphi_D, \varepsilon)}_{d} \right].$$

187

188   The elements of R are vectors of size four, and each contains the number of A, C, G and T bases mapped

189   to this site for a particular sample (the pileup data). The specific element $\boldsymbol{R_A}$ represents base counts from

190   the ancestral strain. $\boldsymbol{R_i}$ and G_i are the base counts and genotype of the i-th descendant lines, respectively,

191   and n is the total number of descendants.

192   The terms labeled "b" and "d" in Equation 3 are the probabilities of the observed sequencing data

193   for a given genotype (i.e. genotype likelihoods). We calculate these genotype likelihoods using a

194   Dirichlet-multinomial (DM) distribution. The DM is a compound distribution in which event-

195   probabilities, $\boldsymbol{p}$, of a multinomial distribution is a Dirichlet-distributed random vector. Using a compound

196   distribution provides flexibility to model the complex sources of error in sequencing data. To make this

197   property of our model explicit, we use a parameterization of the DM distribution where $\boldsymbol{p}$ is a vector of

198   length four containing the expected proportion of reads matching each allele and φ is an overdispersion

199   parameter with values in the interval $[0,1]$. Using this parameterization, the DM distribution is equivalent

200   to a simple multinomial distribution when $\varphi = 0$ and becomes increasingly overdispersed (i.e. the

201   variance increases) as φ tends to 1.

9

202 We demonstrate the calculation of genotype likelihoods using the term for the ancestral genotype

203 in Equation 3 ("b" term) as an example. To calculate $P(\boldsymbol{R_A}|\ G_A;\ \varphi_A, \varepsilon)$, we use the probability mass

204 function of the DM distribution

205 (4)

206
$$P(\boldsymbol{R_A} = \boldsymbol{r}\mid G_A = g;\ \varphi_A, \varepsilon) = \binom{N}{\boldsymbol{r}} \frac{\Gamma(\omega_A)}{\Gamma(\omega_A + N)} \prod_b \frac{\Gamma(\boldsymbol{p_b}\omega_A + \boldsymbol{r_b})}{\Gamma(\boldsymbol{p_b}\omega_A)}.$$

207 Here N is the total number of reads, $\binom{N}{\boldsymbol{r}}$ is the multinomial coefficient, Γ is the gamma function, and

208 $\omega_a = (1 - \varphi_A)/\varphi_A$. The parameter vector $\boldsymbol{p}$ contains the expected frequency of bases in {A, C, G, T} for

209 the site under consideration and is indexed by b. Values in $\boldsymbol{p}$ are determined by both the probability of

210 sequencing error (ε) and the ancestral diploid genotype $g = \{g_1, g_2\}$ following Equation 5.

211 (5)

212
$$\boldsymbol{p_b} = \begin{cases} 1 - \varepsilon, & \text{if } b = g_1 = g_2 & \text{(homozygous match)} \\ \dfrac{1}{2} - \dfrac{\varepsilon}{3}, & \text{if } b = g_1 \neq g_2 \text{ or } b = g_2 \neq g_1 & \text{(heterozygous match)} \\ \dfrac{\varepsilon}{3}, & \text{otherwise} & \text{(error / mismatich)} \end{cases}$$

213

214 We now consider the remaining terms in Equation 3. The term labeled "a" represents the prior

215 probability that the ancestor had a particular genotype (g_A below) at the site under consideration given the

216 nucleotide composition of the *T. thermophila* genome and average heterozygosity of the ancestral strain.

217 We calculate this via a finite-sites model with parent-independent mutation,

218 (6)

219
$$P(G_A = g_A; \theta, \boldsymbol{\pi}) = \begin{cases} \pi_{b_1} \dfrac{1}{1+\theta} + \pi_{b1}\pi_{b2} \dfrac{\theta}{1+\theta} & \text{if } g_1 = g_2 = b_1 & \text{(homozygote)} \\ 2\,\pi_{b_1}\pi_{b_2} \dfrac{\theta}{1+\theta} & \text{if } g_1 = b_1 \text{ and } g_2 = b_2 & \text{(heterozygote)} \end{cases}.$$

220

10

221   Here $\frac{1}{1+\theta}$ is the probability that the ancestor is autozygous at a site, and $\boldsymbol{\pi}$ is the vector of stationary

222   nucleotide/allele frequencies in ancestral genome and b_1 and b_2 refer to the indices of the g_1 and g_2

223   alleles. See Wright (1949) for more details on this model and its biological assumptions.

224   To complete Equation 3 we need to consider the term labeled "c", which represents the

225   probability that the *i*-th MA line inherited a particular genotype, given the ancestral genotype and the

226   probability of mutation. We calculate this via the Felsenstein (1981) model of nucleotide substitution.

227   This model incorporates equilibrium nucleotide frequencies, allowing us to include the extreme AT-bias

228   present in the *T. thermophila* genome.

229   Using the approach described above, we used Equation 2 to calculate both the probability of at

230   least one point-mutation and the probability of exactly one point-mutation at every site along the *T.*

231   *thermophila* reference genome. In MA experiments, multiple mutations at the same site are unlikely;

232   therefore, sites that contain a strong signal of more than one mutation are likely false positives due to

233   systematic errors in sequencing and mapping of reads.

234   This model is implemented in a C++ program called accuMUlate, which makes use of the

235   Bamtools (Barnett et al. 2011) library. The source code used to perform the calculations described above

236   is available under an MIT license from https://github.com/dwinter/accumulate; the specific version of the

237   code used in these analyses is archived at http://dx.doi.org/10.5281/zenodo.19942. We ran our model on a

238   genomic alignment produced by using Bowtie version 2.1.0 (Langmead and Salzberg 2012) to map reads

239   to the December 2011 release of the *T. thermophila* macronuclear genome from the *Tetrahymena*

240   Genome Database (Stover et al. 2006). One site in the reference contained a gap character, which we

241   removed since our reads indicated that it was an artifact. We processed the resulting alignments to remove

242   sequencing and mapping artifacts that could lead to false-positive mutation calls. In particular, we

243   identified and marked duplicate reads using the MarkDuplicates tool from Picard 1.106

244   (http://pricard.sourceforge.net) and performed local realignment around potential indels using GATK 3.2

245   (DePristo et al. 2011; McKenna et al. 2010). We adjusted raw base quality scores by running GATK's

246   BaseRecalibrator tool, using a set of putative single nucleotide variants detected with SAMtools mpileup

247   as input (Li et al. 2009).

248   The putative mutations from this approach were preliminarily identified by running accuMUlate

249   to identify sites with a mutation probability > 0.1 with parameter-values: $\varphi_A = \varphi_D = 0.001$, $\varepsilon = 0.01$,

250    $\mu = 10^{-8}$, $\theta = 0.0001$ and only considering reads with Phred-scaled mapping and base quality scores $\geq$

251   13 (corresponding to an estimated 5% probability of error). The validation phase showed that false-

252   positive mutations were frequently associated with poorly-mapped reads, low coverage regions

253   surrounding deletions with respect to the reference genome, or the presence of rare bases in all samples.

254   Thus, we re-ran the accuMUlate model, excluding all reads with a mapping quality < 25 (corresponding

255   to an estimated 0.3% chance of error), and using the overdispersion parameters $\varphi_A = 0.03$ and $\varphi_D =$

256   0.01. Setting $\varphi_A > \varphi_D$ allowed us to accommodate the increased variance generated by sequencing

257   pooled genomic exclusion lines to infer the ancestral genotype. In addition, we filtered out putative

258   mutations that were not supported by at least 3 reads in both forward and reverse orientation. This final

259   filtering step removed sites with unusually low coverage and those displaying strand bias, both

260   characteristics associated with mismapped reads. We investigated the influence of our over-dispersion

261   parameters by calculating the overall likelihood of the data using the initial and final parameter values. In

262   order to make these results directly comparable, these calculations were performed on a data set

263   consisting of all bases with quality score ≥ 13 from reads with a mapping quality ≥ 25.

264   **Validation of putative mutations**

265   The validity of a subset of putative mutations was tested by Sanger sequencing. All mutations identified

266   by either the consensus or the probabilistic approach were tested with suitable primers up to 500 bp away

267   from the mutation site. Primers were designed using the default parameters of Primer3 (Koressaar and

12

268   Remm 2007; Untergrasser et al. 2012) as implemented in Geneious (Kearse et al. 2012). Successful PCR

269   products were purified and directly sequenced at Lone Star Labs (Houston, TX).

Mutation rate calculations

271   Our probabilistic approach to mutation detection also provides a way to calculate the number of sites at

272   which we could have detected a mutation if one was present, and thus the correct denominator to use for

273   mutation rate calculations. Using our final model parameters, we shuffled the vector of read-counts

274   generated from a given sample in order to simulate mutations in our data. This procedure was repeated for

275   every site in the reference genome, shuffling the read counts from each descendent separately then

276   recalculating the probability of a mutation. A site was treated as missing from a sample if the mutation

277   probability calculated from shuffled read-counts was < 0.1 or if the most probable mutant allele was not

278   supported by at least 3 reads in both the forward and the reverse orientation. To investigate the impact of

279   our final parameter values and filtering criteria on the number of callable sites we repeated this procedure

280   using the initial parameter set (i.e. with $\varphi_A = \varphi_D = 0.001$ and removing reads with mapping quality $<$

281   13). The number of callable sites detected using this approach for each line is given in Table 1.

282   We calculated the mutation rate by summing the number of validated mutations (n_i) across MA

283   lines, and then dividing it by the product of the number of analyzed sites (L) and the number of

284   generations (T) in each MA line (i): $\hat{\mu} = \sum_i n_i / (L\,T)$. Assuming that the number of mutations in each line

285   follows a Poisson distribution (but not necessarily the same distribution) and ignoring uncertainty in our

286   estimates for L and T, the standard error for our estimate of mutation rate was estimated as $SE(\hat{\mu}) =$

287    $\sqrt{\hat{\mu}/(L\,T)}$, and a 95% confidence interval was constructed as $\hat{\mu} \pm 1.96\,SE(\hat{\mu})$. We also performed the

288   same calculation on log-transformed values of $\hat{\mu}$, L, and, T to produce a "log-space" confidence interval.

289   To calculate genomic mutation rates we assumed a haploid genome size of 104 Mb (Eisen et al. 2006).

13

290 **Annotation of mutations**

291 We annotated the functional context of identified mutations using snpEff (Cingolani et al. 2012) and the

292 December 2011 release of the *T. thermophila* macronuclear genome annotation file from the *Tetrahymena*

293 Genome Database.

294 RESULTS

295 **Mutation detection and validation**

296 To estimate the micronuclear mutation rate, we sequenced the whole macronuclear genomes of 10

297 homozygous genomic-exclusion lines, each derived from a separate *T. thermophila* line that had

298 undergone MA for approximately 1000 generations. Using two different mutation-detection approaches (a

299 widely used "consensus" method and a new probabilistic approach described in the Materials and

300 Methods), we identified 92 sites for which there was some evidence of a mutation in at least one lineage.

301 On closer inspection we found an unusual pattern — more than half of the apparent mutations were from

302 lines M47 and M51, and in many cases reads containing the apparent mutant allele from one of these lines

303 were also sequenced from the other line (but absent or very rare in all other lines).

304   To investigate this anomaly further we analyzed the frequency of non-reference bases in all

305 samples across the whole genome (Supplementary Data). These analyses demonstrated that M47 and M51

306 differ from all other lines in the frequency of non-reference bases and in patterns of sequencing coverage.

307 We do not know what caused the anomaly. It is possible that some cellular process occurred in these lines

308 but not others (e.g., the incorporation of sequences usually restricted to the micronucleus, or the inclusion

309 of DNA from the B* strain during genomic exclusion). It is extremely unlikely that M47 and M51

310 independently accrued more shared mutations than independent mutations during our MA experiment.

311 For this reason, we have excluded these lines from all subsequent analyses.

14

312   Forty putative mutations remained after lines M47 and M51 were removed (Supplementary Table

313   S2). We attempted to validate each of these mutations using Sanger sequencing. Only 4 of these

314   mutations were validated. The remaining sites were either shown to be false positives (11 sites) or failed

315   to generate either PCR amplicons or clean sequence traces (25 sites). Closer inspection of the data

316   underpinning both the false positive and inconclusive mutations showed these sites to have unusually low

317   sequencing coverage and low mapping quality, and to be subject to strand bias. All of these properties are

318   associated with mapping error, and are known to generate false positive variant calls (Li 2014). For this

319   reason, we re-ran our probabilistic mutation caller using stricter filters for mapping quality and excluding

320   putative mutations that did not have at least 3 sequencing reads supporting a mutation in both the forward

321   and reverse orientation. None of the inconclusive or false positive sites were called as mutations in this

322   analysis, which also detected an additional mutation that was confirmed by Sanger sequencing. Thus, we

323   detected a total of 5 mutations across 8 MA lines, with no line having more than one confirmed mutation

324   (Table 1). Our probabilistic method produced more false positives than the consensus approach but

325   generated no false negatives (Supplementary Table S2). Of the 5 mutations detected, 2 are non-

326   synonymous, 2 are synonymous, and one is in an intergenic region.

327   **Number of callable sites**

328   We estimated the denominator for our mutation rate estimates by calculating the number of sites at which

329   a mutation could be called if one was present. An average of 86.1% of the reference genome was callable

330   per line (Table 1). Sites for which we lacked power to detect mutations in at least one line are in relatively

331   gene-poor regions; 30% of such sites are in exons compared to 49% of always-included sites. We also

332   considered the impact of our final filtering steps and model parameters on our analyses. The more

333   stringent filtering steps we used to generate our final mutation set reduced the proportion of callable sites

334   per line, with the median proportion of callable sites declining from 93% to 88% (Table 1). The final

335   overdispersion values used in our probabilistic mutation caller produced a better fit to our data than the

336   initial values, with the overall log likelihood improving by 8×10^4.

15

337 **Mutation rate**

338 Given the number of callable sites, the 5 mutations that we detected yield a base-substitution mutation

339 rate estimate of 7.61×10^{-12} per base pair per asexual generation (95% confidence interval, CI = [$0.691 \times$

340 10^{-12}, 14.53×10^{-12}] using the standard method or [4.68×10^{-12}, 12.38×10^{-12}] using log-transformed

341 values). This point estimate is approximately one third of the rate reported for *P. tetraurelia*, although the

342 95% CIs of both estimates overlap (fig. 1), and equates to a genome-wide rate of 0.8 base-substitution

343 mutations per haploid genome per thousand asexual generations (95% CI = [0.07, 1.50]).

344   If our estimate of the base-substitution mutation rate holds for the portions of the genome from

345 which we did not have sufficient power to detect mutations, then we estimate that we have failed to detect

346 an additional 0.87 mutations across all of the macronuclear genomes sequenced.

347 DISCUSSION

348 We have used whole-genome sequencing and a novel mutation-detection approach to estimate the base-

349 substitution mutation rate of *T. thermophila* from 8 MA lines (Long et al. 2013) and obtained an estimate

350 of 7.61×10^{-12} mutations per-site per-generation. This is the lowest estimate of base-substitution mutation

351 rate from a eukaryote (for surveys of mutation-rate estimates see fig. 1 and Sung et al 2012b), and indeed

352 lower than that observed in any prokaryote. However, it is not significantly different from the rate in

353 either the social amoeba *Dictyostelium discoideum* (Saxer et al. 2012) or the ciliate *P. tetraurelia* (Sung et

354 al. 2012b). The fact that the two lowest mutation rates have been recorded in ciliates supports the

355 hypothesis that ciliates in general have low germline mutation rates (Sung et al. 2012b).

356   Direct estimates of the mutation rate from MA lines can only be as accurate as the methods used

357 to detect mutations. Our estimate of a low mutation rate in *T. thermophila* could conceivably result from a

358 high rate of false-negative results. However, we believe that this is unlikely. Our approach to mutation

359 detection was designed to maximize the sensitivity of our analyses. We initially applied lenient filters to

16

360   our data and attempted to validate all putative mutations detected by two separate methods. Most of the

361   putative mutations suggested by this initial analysis could not be validated by Sanger sequencing. For this

362   reason, we developed filters and model-parameters that improved the specificity of our mutation-calling

363   method (producing negligible mutation probabilities for all of our unconfirmed mutations, while still

364   supporting our confirmed mutations). It is possible that this increased stringency also led us to miss

365   mutations present in our descendant lines. To account for the possibility of such false negatives in our

366   mutation rate estimates, we simulated mutations in our data. This allowed us to identify sites at which we

367   would not be able to detect a mutation in a given line even if one was present. Sites for which we could

368   not call a simulated mutation were not included in the denominator of our mutation rate calculation. Thus,

369   we are confident that our mutation rate estimate is accurate, at least for the regions of the genome from

370   which we could call mutations.

371   Our mutation rate estimate allows us to estimate the effective population size of *T. thermophila*.

372   If we assume that silent sites in protein-coding genes are effectively neutral and under drift-mutation

373   equilibrium, the population-level heterozygosity at silent sites (π_s) has expected value $4N_e\mu$, where N_e is

374   the effective population size, and μ is mutation rate per site per generation. Using the estimate $N_e \times \mu = 8$

375    $\times 10^{-4}$ reported by Katz et al. (2006), if we assume that mutation rates in the germline and somatic

376   genomes are equal, our N_e estimate for *T. thermophila* is 1.12×10^8, which is almost identical to that of *P.*

377   *tetraurelia* (N_e=1.24×10^8; Sung et al. 2012b). These estimates may seem surprising given the

378   observations that *P. tetraurelia* is cosmopolitan and regularly isolated from different continents (Catania

379   et al. 2009), while *T. thermophila* has a distribution limited to the eastern United States (Zufall et al.

380   2013). However, the relationship between census population size and genetic diversity (and therefore

381   estimated N_e) is not a simple one (Leffler et al. 2012; Lewontin 1974). In very large populations

382   stochastic processes, including demographic events that prevent populations from reaching mutation-drift

383   equlibrium (Haigh and Maynard Smith 1972; Leffler et al. 2012) and the effects of selection on sites

384   linked to neutral variants (Gillespie 2001; Lynch 2007; Neher et al. 2013), limit genetic diversity across

17

385   the whole genome. Regardless, the large effective population size estimated here suggests that selection

386   will have considerable power in the evolution of *T. thermophila*.

387   The unusual genome structure and life history of ciliates may explain their low mutation rates.

388   Sung et al. (2012a) argued that mutation rates are minimized to the extent made possible by the power of

389   natural selection — the "drift barrier" hypothesis. Selection operates to reduce the mutation rate based on

390   the "visible" mutational load, and mutations that accumulate in the germline genome in ciliates during

391   asexual generations are not expressed and exposed to selection until they are incorporated in a new

392   somatic genome following sexual reproduction. Thus, the mutation rate per selective event is equal to the

393   mutation rate per asexual generation multiplied by the number of asexual generations between rounds of

394   sexual reproduction. The low mutation rates reported for ciliates may have evolved naturally as a

395   consequence of the many asexual generations in between bouts of sexual reproduction, combined with

396   large effective population sizes that promote strong selection for low mutation rates.

397   Unlike *P. tetraurelia*, *T. thermophila* does not undergo senescence in the absence of sex, and we

398   lack a good estimate for the frequency of sexual reproduction in natural populations (Doerder et al. 1995).

399   Therefore, we cannot put an upper bound on the number of asexual generations between conjugation

400   events. However, we can estimate a lower bound because cells arising from sexual reproduction enter a

401   period of immaturity lasting ~50–100 divisions (Lynn and Doerder 2012). We know that the germline

402   genome divides at least this many times without opportunity for selection on any newly acquired

403   mutations. Using the immaturity period as a proxy for the frequency of sex gives an estimate of the base-

404   substitution mutation rate of ~0.1 mutations per haploid genome per conjugation event — much closer to

405   that of other eukaryotes per round of DNA replication (Sung et al. 2012b).

406   Most mutations with effects on fitness are deleterious, so the accumulation of mutations in the

407   absence of selection is expected to lead to a reduction in organismal fitness (Bateman 1959; Halligan and

408   Keightley 2009; Mukai 1964; Muller 1928). The fitness of a genomic exclusion line derived from an MA

18

409   line of *T. thermophila* should, in part, reflect the germline mutations in that MA line. If most germline

410   mutations are base-substitutions, the low germline base-substitution rate would lead us to predict modest

411   effects on the fitness of the genomic exclusion lines we studied. Surprisingly, some of these lines

412   experienced substantial fitness losses relative to the ancestor (Long et al. 2013). For example, we did not

413   detect any base-substitution mutations in the line with largest observed loss in fitness (M50, w=0.38)

414   (Table 1). It is unlikely that the fitness losses observed in these MA lines can be explained by other

415   undetected single-base substitutions, as our mutation calling method had power to detect mutations in an

416   average of 86.1% of the genome (Table 1) and the excluded portion of the genome is relatively gene poor.

417   Rather, it seems likely the fitness of these lines is determined in part by indels and other structural

418   variants that we did not include in this study. Furthermore, non-Mendelian patterns of inheritance could

419   obscure the relationship between mutations and fitness. For example, the fitness of an individual line may

420   be influenced by epigenetic processes, such as cortical inheritance (Sonneborn 1963) or small RNA

421   guided genome rearrangement (Mochizuki and Gorovsky 2004).

422   Our probabilistic mutation calling method can directly model the overdispersion produced by

423   modern sequencing techniques. Our initial run of this method used very low values for the overdispersion

424   parameters and produced many false positive mutation calls. We believe that these false positives arose

425   from sites with data that did not fit the expectation of relatively clean data that these low overdispersion

426   values represent. Using data form the validation phase, we were able to show that increasing the

427   overdispersion parameter values (and being more stringent about which sequencing reads were included

428   in our analysis) improved the accuracy of our method such that it produced fewer false positives while

429   still correctly identifying all validated mutations. In addition to improving the accuracy of our mutation

430   calling, increasing the values of the overdispersion parameters substantially increased the fit of our model

431   to the sequencing data. Although the small number of true mutations in this experiment prevents us from

432   performing a more complete analysis, this study demonstrates that modeling overdispersion in sequencing

433   data can improve mutation calling methods.

19

434   In this study we have established that it is possible to detect mutations in *T. thermophila* MA

435   lines through short-read sequencing, and thus to directly study the nature of mutation in this model

436   organism. Although we were able to show that *T. thermophila* shares a low mutation rate with *P.*

437   *tetraurelia* (the only other ciliate for which a mutation rate has been directly estimated), there is still much

438   to learn about mutation in this species. For instance, the unusual genome structure of ciliates presents a

439   novel test of the drift-barrier hypothesis of mutation rate evolution (Sung et al. 2012a). If the mutation

440   rates of the germline and somatic nuclei can evolve independently then we would expect the somatic

441   mutation rate to be higher (i.e. more similar to the mutation rates of other eukaryotes) because somatic

442   mutations are exposed to selection after each cell division. Furthermore, the small number of mutations

443   accumulated over this experiment has prevented us from analyzing the spectrum of mutations arising in *T.*

444   *thermophila* and determining the influence of mutational biases on genome evolution. Similarly, the few

445   mutations that we detect seem inadequate to explain the observed losses of fitness during MA. Future

446   studies using more MA lines evolving over longer periods and detecting indels and other structural

447   variants accrued during MA will be needed to fully understand the effects of mutation and selection in *T.*

448   *thermophila*.

449

ACKNOWLEDGEMENTS

REFERENCES

Allen SL 1963. Genomic exclusion in *Tetrahymena*: genetic basis. J Protozool. 10: 413–420.

Barnett DW, Garrison EK, Quinlan AR, Strömberg MP, Marth GT 2011. BamTools: a C++ API and toolkit for analyzing and managing BAM files. Bioinformatics 27: 1691–1692.

Bateman AJ 1959. The viability of near-normal irradiated chromosomes. Int J Radiat Biol 1: 170–180.

Behringer MG, Hall DW 2015. Genome-wide estimates of mutation rates and spectrum in *Schizosaccharomyces pombe* indicate CpG sites are highly mutagenic despite the absence of DNA methylation. G3 6: 149–160.

Bruns P, Cassidy-Hanley D 1999. Methods for genetic analysis. Methods Cell Biol 62: 229–240.

Cartwright RA, Hussin J, Keebler JEM, Stone EA, Awadalla P 2012. A family-based probabilistic method for capturing de novo mutations from high-throughput short-read sequencing data. Stat Appl Genet Molec 11: Article 6.

Cingolani P, et al. 2012. A program for annotating and predicting the effects of single nucleotide polymorphisms, SnpEff: SNPs in the genome of *Drosophila melanogaster* strain w1118; iso-2; iso-3. Fly 6: 80–92.

Denver DR, et al. 2009. A genome-wide view of *Caenorhabditis elegans* base-substitution mutation processes. Proc Natl Acad Sci USA 106: 16310–16314.

DePristo MA, et al. 2011. A framework for variation discovery and genotyping using next-generation DNA sequencing data. Nat Genet 43: 491–498.

Doerder FP 2014. Abandoning sex: multiple origins of asexuality in the ciliate *Tetrahymena*. BMC Evol Biol 14: 112.

Doerder FP, Gates MA, Eberhardt FP, Arslanyolu M 1995. High frequency of sex and equal frequencies of mating types in natural populations of the ciliate *Tetrahymena thermophila*. Proc Natl Acad Sci USA 92: 8715–8718.

Eisen JA, et al. 2006. Macronuclear genome sequence of the ciliate *Tetrahymena thermophila*, a model eukaryote. PLoS Biol 4: e286.

Farlow A, et al. 2015. The spontaneous mutation rate in the fission yeast *Schizosaccharomyces pombe*. Genetics 201: 737–744.

Felsenstein J 1981. Evolutionary trees from DNA-sequences - a maximum-likelihood approach. J Mol Evol 17: 368–376.

Gillespie JH 2001. Is the population size of a species relevant to its evolution? Evolution 55: 216–219.

Gorovsky M, Yao M, Keevert J, Pleger G 1975. Isolation of micro- and macronuclei of *Tetrahymena pyriformis*. Methods Cell Biol 9: 311–327.

Haigh J, Maynard Smith J 1972. Population size and protein variation in man. Genet Res 19: 73–89.

Halligan DL, Keightley PD 2009. Spontaneous mutation accumulation studies in evolutionary genetics. Annu Rev Ecol Evol Syst 40: 151–172.

Katz LA, Bhattacharya D. 2006. Genome evolution in eukaryotic microbes. Oxford, UK: Oxford University Press.

Katz LA, Snoeyenbos-West O, Doerder FP 2006. Patterns of protein evolution in *Tetrahymena thermophila*: implications for estimates of effective population size. Mol Biol Evol 23: 608–614.

Kearse M, et al. 2012. Geneious Basic: an integrated and extendable desktop software platform for the organization and analysis of sequence data. Bioinformatics 28: 1647–1649.

Keightley P, Trivedi U, Thomson M, Oliver F, Kumar S et al. 2009. Analysis of the genome sequences of three *Drosophila melanogaster* spontaneous mutation accumulation lines. Genome Res 19: 1195–1201.

Keightley PD, Ness RW, Halligan DL, Haddrill PR 2014. Estimation of the spontaneous mutation rate per nucleotide site in a *Drosophila melanogaster* full-sib family. Genetics 196: 313–320.

Koressaar T, Remm M 2007. Enhancements and modifications of primer design program Primer3. Bioinformatics 23: 1289–1291.

Langmead B, Salzberg SL 2012. Fast gapped-read alignment with Bowtie 2. Nat Methods 9: 357–359.

Lee H, Popodi EM, Tang H, Foster PL 2012. Rate and molecular spectrum of spontaneous mutations in the bacterium *Escherichia coli* as determined by whole-genome sequencing. Proc Natl Acad Sci USA 109: E2774–E2783.

Leffler EM, et al. 2012. Revisiting an old riddle: what determines genetic diversity levels within species? PLoS Biol 10: e1001388.

Lewontin RC. 1974. The genetic basis of evolutionary change. New York, USA: Columbia University Press.

Li H 2014. Toward better understanding of artifacts in variant calling from high-coverage samples. Bioinformatics 30: 2843–2851.

Li H, Durbin R 2009. Fast and accurate short read alignment with Burrows-Wheeler Transform. Bioinformatics 25: 1754–1760.

Li H, et al. 2009. The sequence alignment/map (SAM) format and SAMtools. Bioinformatics 25: 2078–2079.

Lind PA, Andersson DI 2008. Whole-genome mutational biases in bacteria. Proc Natl Acad Sci USA 105: 17878–17883.

Long H, Paixao T, Azevedo RBR, Zufall RA 2013. Accumulation of spontaneous mutations in the ciliate *Tetrahymena thermophila*. Genetics 195: 527–540.

Long H, et al. 2015. Mutation rate, spectrum, topology, and context-dependency in the DNA mismatch repair (MMR) deficient *Pseudomonas fluorescens* ATCC948. Genome Biol Evol 7: 262–271.

Lynch M. 2007. The origins of genome architecture. Sunderland, MA: Sinauer Associates, Inc.

Lynch M, Sung W, Morris K, Coffey N, Landry CR, et al. 2008. A genome-wide view of the spectrum of spontaneous mutations in yeast. Proc Natl Acad Sci USA 105: 9272–9277.

Lynn DH, Doerder FP 2012. The life and times of *Tetrahymena*. Methods Cell Biol 109: 9–27.

McKenna A, et al. 2010. The genome analysis toolkit: a MapReduce framework for analyzing next-generation DNA sequencing data. Genome Res 20: 1297–1303.

Mochizuki K, Gorovsky MA 2004. Small RNAs in genome rearrangement in *Tetrahymena*. Curr Opin Genet Dev 14: 181–187.

Mukai T 1964. The genetic structure of natural populations of *Drosophila melanogaster*. I. Spontaneous mutation rate of polygenes controlling viability. Genetics 50: 1–19.

Muller HJ 1928. The measurement of gene mutation rate in *Drosophila*, its high variability, and its dependence upon temperature. Genetics 13: 279–357.

Neher RA, Kessinger TA, Shraiman BI 2013. Coalescence and genetic diversity in sexual populations under selection. Proc Natl Acad Sci U S A 110: 15836–15841.

Ness RW, Morgan AD, Colegrave N, Keightley PD 2012. Estimate of the spontaneous mutation rate in *Chlamydomonas reinhardtii*. Genetics 192: 1447–1454.

Ness RW, Morgan AD, Vasanthakrishnan RB, Colegrave N, Keightley PD 2015. Extensive *de novo* mutation rate variation between individuals and across the genome of *Chlamydomonas reinhardtii*. Genome Res 25: 1739–1749.

Ossowski S, et al. 2010. The rate and molecular spectrum of spontaneous mutations in *Arabidopsis thaliana.* Science 327: 92–94.

Saxer G, et al. 2012. Whole genome sequencing of mutation accumulation lines reveals a low mutation rate in the social amoeba *Dictyostelium discoideum*. PLoS One 7: e46759.

Sonneborn TM. 1963. Does preformed cell structure play an essential role in cell heredity? In: Allen JM, editor. The nature of biological diversity. New York: McGraw-Hill.

Stover NA, et al. 2006. *Tetrahymena* Genome Database (TGD): a new genomic resource for *Tetrahymena thermophila* research. Nucleic Acids Res 34: D500–D503.

Sung W, et al. 2015. Asymmetric context-dependent mutation patterns revealed through mutation-accumulation experiments. Mol Biol Evol 32: 1672–1683.

Sung W, Ackerman MS, Miller SF, Doak TG, Lynch M 2012a. Drift-barrier hypothesis and mutation rate evolution. Proc Natl Acad Sci USA 109: 18488–18492.

Sung W, et al. 2012b. Extraordinary genome stability in the ciliate *Paramecium tetraurelia*. Proc Natl Acad Sci USA 109: 19339–19344.

Untergrasser A, et al. 2012. Primer3 - new capabilities and interfaces. Nucleic Acids Res 40: e115.

Wright S 1949. The genetical structure of populations. Ann Hum Genet 15: 323–354.

Zhu YO, Siegal ML, Hall DW, Petrov DA 2014. Precise estimates of mutation rate and spectrum in yeast. Proc Natl Acad Sci USA 111: E2310–E2318.

Zufall RA, Dimond KL, Doerder FP 2013. Restricted distribution and limited gene flow in the model ciliate *Tetrahymena thermophila*. Mol Ecol 22: 1081–1091

FIGURE LEGENDS
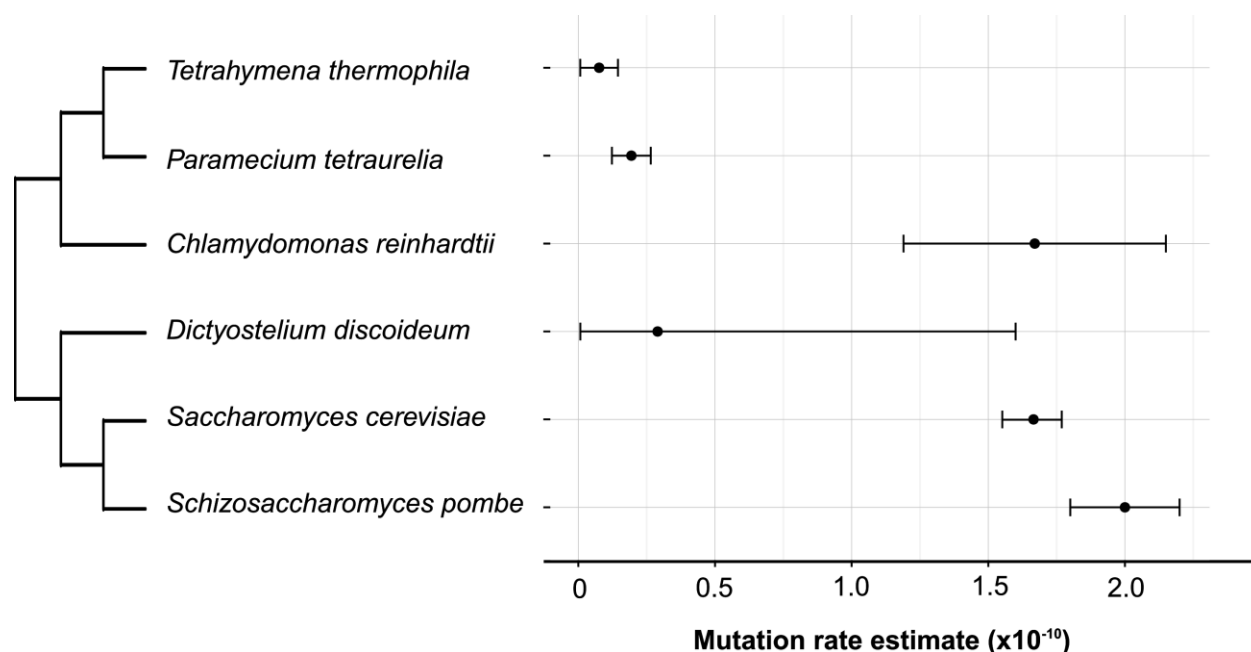
FIG. 1.—Mutation rate estimates for unicellular eukaryotes. Base-substitution mutation rates per nucleotide per generation estimated for different unicellular eukaryotes: *T. thermophila* (this paper), *P. tetraurelia* (Sung et al. 2012b), *C. reinhardtii* (Ness et al. 2015), *D. discoideum* (Saxer et al. 2012), *Sa. cerevisiae* (Zhu et al. 2014), and *Sc. pombe* (Farlow et al. 2015). The phylogenetic tree was retrieved from the Open Tree of Life (Hinchliff et al. 2015); branch lengths are arbitrary. Error bars are 95% confidence intervals calculated by ignoring uncertainty in the number of sites at which a mutation could be detected and the number of generations that each MA ran experiment ran for.
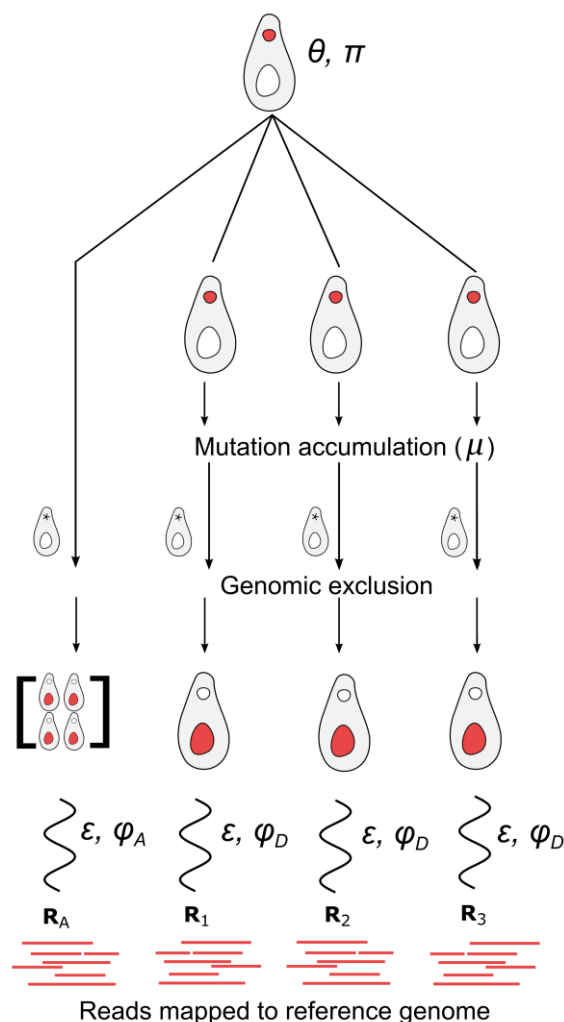
FIG. 2.—Experimental design in relation to parameters of probabilistic mutation-detection model. A complete description of the experiment is presented in Long et al. (2013). Here, we describe how the experiment relates to the parameters used in our probabilistic mutation-calling model. Specifically, the ancestral line with average heterozygosity θ and genome-wide nucleotide frequencies π is used to generate a set of MA lines. Each of these lines accumulates mutations at a rate μ per nucleotide-site per generation for 1000 generations. Genomic exclusion, an auto-diploidization process, is used to generate lines with macronuclei representing one haploid-copy of each MA line (and multiple copies of the ancestral line, in order to detect ancestral heterozygosity). The macronuclear genomes of these genomic exclusion lines are then sequenced with a sequencing error rate of ε and overdispersion caused by library

preparation and other correlated errors modeled as φ_A and φ_D for ancestral and descendant lines

respectively. A full description of this model and its parameters is given in the subsection of the Materials

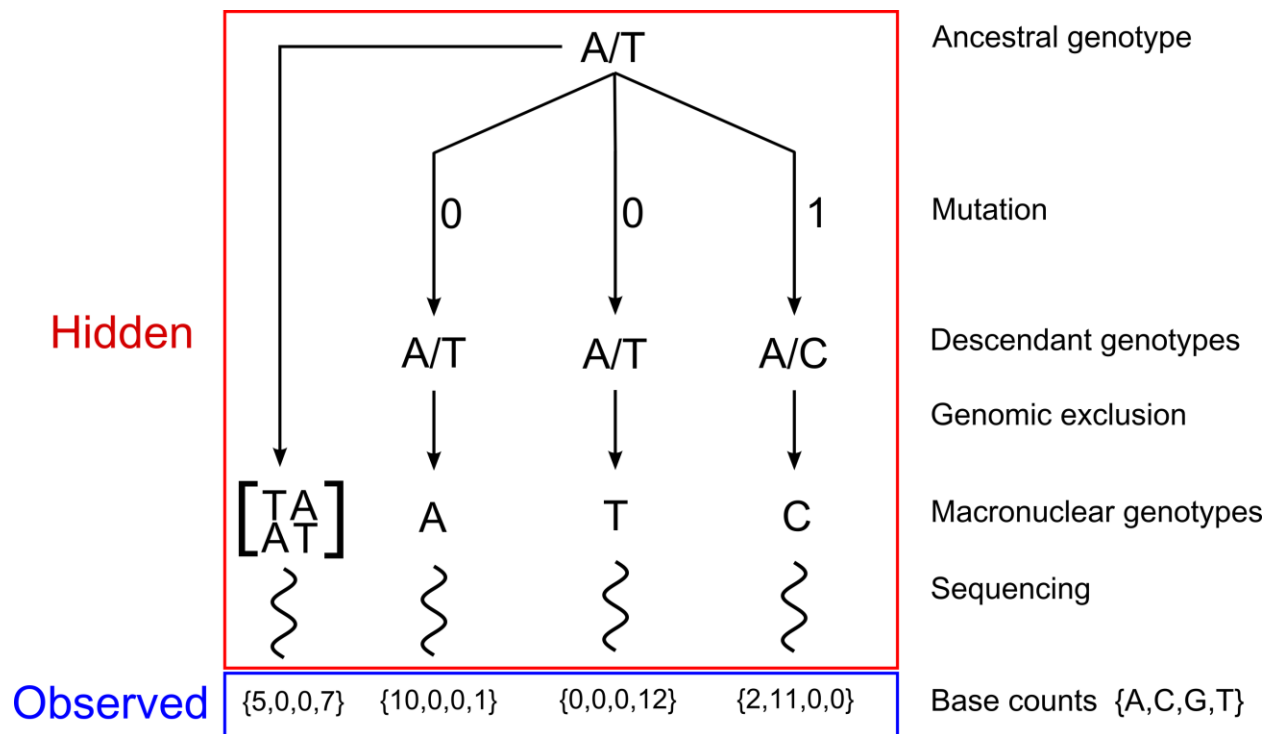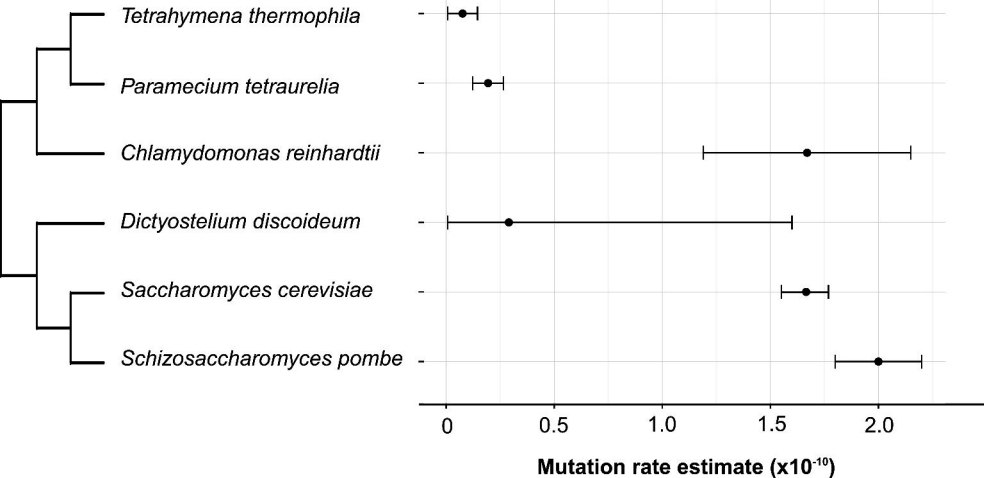and Methods labeled "Probabilistic approach using accuMUlate"

FIG. 3.—Illustration of a single history in the accuMUlate method. In our model, a history is a unique combination of states (i.e. the genotypes of ancestral and MA lines, results of genomic exclusions and errors introduced during sequencing) generated during an MA experiment. Here we illustrate one such history by giving values to the different states in a model reflecting the same experimental design as fig. 2 and show how we calculate the probability that this history occurred and generated the observed sequencing data. Because we treat sites in the reference genome independently, we describe the process for a single site. Specifically, we consider a history in which an ancestor that is heterozygous with genotype A/T is used to establish three MA lines. One of those lines experiences a mutation from A/T to A/C, and the C allele of this mutant is passed on to a new macronuclear genome through genomic exclusion. The only data we observe for this locus is the set of bases mapped to this site that pass our filtering steps. We represent this data as vectors containing the number of A, C, G and T bases mapped to a given site (the base counts). We can use Equation 3 to calculate the probability that this sequencing data was generated by the specific history shown here. To do this, we first calculate the probability that the
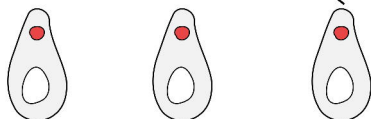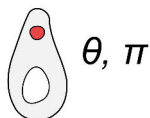
ancestor would have genotype A/T and that the observed sequencing data from the ancestor could be generated from this genotype (using Equations 6 and 4, respectively). Next, we consider the MA (descendant) lines, calculating the probability that the three descendant lines would have genotypes A, T and C and that the observed sequencing data could be generated from these genotypes. In this case we use the Felsenstein (1981) model of nucleotide substitution to calculate the probabilities that genomic exclusions generated from the MA lines would have these genotypes. We use the same genotype likelihood model (Equation 4) to calculate the probability that the sequencing data was generated from MA lines with these genotypes. Because each of the descendant lines is independent of each other, the overall probability of the history is simply the product of the probabilities for the ancestral and all descendant lines (Equation 3). We calculate the probability of a site containing at least one mutation by repeating this procedure for all possible histories at a given site (i.e. all possible combinations of genotypes) and keeping track of those histories that contain one or more mutations (Equation 2)

Line	Coverage	Generations	Fitness[a]	Callable[b]		Mutation				
				Initial	Final	Scaffold	Substitution	Feature	Locus	Effect
M5	64.17	1000	0.56	0.92	0.88	scf_8254658	g.334881C>T	Exon	TTHERM_00675900A	Synonymous (gaC>gaT, D>D)
M19	53.05	1000	0.64	0.93	0.88	-	-	-	-	-
M20	34.42	1000	0.44	0.93	0.88	scf_8254594	g.239327A>T	Intron	TTHERM_00286840A	-
M25	30.88	1000	0.57	0.93	0.88	scf_8254607	g.179325C>T	Exon	TTHERM_00439220A	Non Synonymous (Gtt>Att, V>I)
M28	50.65	200	0.65	0.92	0.87	-	-	-	-	-
M29	31.36	1000	0.49	0.93	0.88	scf_8254365	g.304140T>G	Intergenic	-	-
M40	16.84	1000	0.57	0.83	0.63	scf_8254002	g.27830G>A	Exon	TTHERM_01128590A	Non Synonymous (tGT>tAt, C>Y)
M50	106.65	1000	0.38	0.93	0.88	-	-	-	-	-

a. Fitness data from Long et al. (2013), using exponential growth rate as fitness metric and normalized by dividing the ancestral growth rate.
b. The proportion of all sites in the MAC genome (1.04Mb) from which a mutation could have been called if one was present. "Initial" refers to the first analysis (with reads with mapping quality < 13 removed and parameter values $\varphi_A = 0.001, \varphi_D = 0.001$), "final" refers to the subsequent analysis (with reads with mapping quality < 30 removed and putative mutations supported by < 3 read in forward and reverse orientation removed, and with parameter values $\varphi_A = 0.03, \varphi_D = 0.01$).

Table 1: Summary of sequencing data and detected mutations. Note, no mutations were detected from lines M50, M28 or M19.
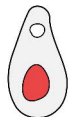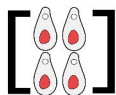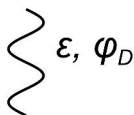
Mutation rate estimate (x10⁻¹⁰)
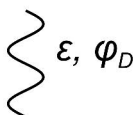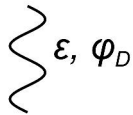
Reads mapped to reference genome

Hidden

Observed

A/T — Ancestral genotype

0   0   1 — Mutation

A/T   A/T   A/C — Descendant genotypes

— Genomic exclusion

$\begin{bmatrix} T & A \\ A & T \end{bmatrix}$ A   T   C — Macronuclear genotypes

— Sequencing

{5,0,0,7}   {10,0,0,1}   {0,0,0,12}   {2,11,0,0} — Base counts {A,C,G,T}